Will atmospheric neutrino experiment at Hyper-Kamiokande see non-standard interaction effects?

Osamu Yasuda

Department of Physics, Tokyo Metropolitan University,
Hachioji, Tokyo 192-0397, Japan

In this talk we discuss the possibility to test the hypothesis, which has been proposed to explain the tension between the mass-squared differences of the solar neutrino and KamLAND experiments by the non-standard flavor-dependent interaction in neutrino propagation, with the atmospheric neutrino observations at the future Hyper-Kamiokande experiment.

1 Introduction

In the standard three flavor framework, neutrino oscillations are described by the mixing matrix

$$U = \begin{pmatrix} c_{12}c_{13} & s_{12}c_{13} & s_{13}e^{-i\delta} \\ -s_{12}c_{23} - c_{12}s_{23}s_{13}e^{i\delta} & c_{12}c_{23} - s_{12}s_{23}s_{13}e^{i\delta} & s_{23}c_{13} \\ s_{12}s_{23} - c_{12}c_{23}s_{13}e^{i\delta} & -c_{12}s_{23} - s_{12}c_{23}s_{13}e^{i\delta} & c_{23}c_{13} \end{pmatrix},$$

where the notations are as follows: $c_{ij} \equiv \cos\theta_{ij}$, $s_{ij} \equiv \sin\theta_{ij}$ and θ_{ij} $(j,k) = (1,2),(1,3),(2,3)$ are the three mixing angles and δ is the CP phase. Thanks to the successful results of the solar, atmospheric, reactor and accelerator neutrino experiments, the three mixing angles and the two mass squared differences have been measured. The currently unknown quantities are the mass hierarchy pattern $(\text{sign}(\Delta m_{31}^2))$, the octant of θ_{23} $(\text{sign}(\pi/4 - \theta_{23}))$ and δ. It is expected that these unknown quantities will be measured by the neutrino experiments in the future, particularly those with intense accelerator neutrino beams[1, 2]. These future experiments are expected to probe new physics beyond the standard model with massive neutrinos, from the deviation from the standard scheme.

In the standard three flavor framework of neutrinos, the Dirac equation for the flavor eigenstate $\Psi^T \equiv (\nu_e, \nu_\mu, \nu_\tau)$ of neutrino in matter is given by

$$i\frac{d\Psi}{dt} = \left[U\text{diag}\,(E_1, E_2, E_3)\,U^{-1} + \mathcal{A} \right]\Psi. \tag{1}$$

Here the matter potential $\mathcal{A}$ is given by

$$\mathcal{A} = A \begin{pmatrix} 1 & 0 & 0 \\ 0 & 0 & 0 \\ 0 & 0 & 0 \end{pmatrix}. \tag{2}$$

$A \equiv \sqrt{2}G_F n_e$ stands for the standard matter effect which comes from the charged current interaction, n_e is the number density of the electron in the matter.

It was pointed out in Ref. 4 that there is a tension between the mass-squared difference deduced from the solar neutrino observations and the one from the KamLAND experiment, and

that the tension can be resolved by introducing the flavor-dependent NSI in neutrino propagation. Such a hint for NSI gives us a strong motivation to study NSI in propagation in details.[a]

The flavor-dependent nonstandard four-fermi interactions which is discussed in this talk are given by

$$\mathcal{L}_{\text{eff}}^{\text{NSI}} = -2\sqrt{2}\,\epsilon_{\alpha\beta}^{fP} G_F (\overline{\nu}_\alpha \gamma_\mu P_L \nu_\beta)\,(\overline{f}\gamma^\mu P f), \tag{3}$$

where only the interactions with $f = e, u, d$ are relevant to the flavor transition of neutrino due to the matter effect, G_F denotes the Fermi coupling constant, P stands for a projection operator and is either $P_L \equiv (1 - \gamma_5)/2$ or $P_R \equiv (1 + \gamma_5)/2$. In the presence of these interactions (3), the matter potential is modified to

$$\mathcal{A} = A \begin{pmatrix} 1 + \epsilon_{ee} & \epsilon_{e\mu} & \epsilon_{e\tau} \\ \epsilon_{e\mu}^* & \epsilon_{\mu\mu} & \epsilon_{\mu\tau} \\ \epsilon_{e\tau}^* & \epsilon_{\mu\tau}^* & \epsilon_{\tau\tau} \end{pmatrix}, \tag{4}$$

where $\epsilon_{\alpha\beta}$ are defined as $\epsilon_{\alpha\beta} \equiv \sum_{f,P}(n_f/n_e)\epsilon_{\alpha\beta}^{fP} \simeq \sum_P \left(\epsilon_{\alpha\beta}^{eP} + 3\epsilon_{\alpha\beta}^{uP} + 3\epsilon_{\alpha\beta}^{dP}\right)$, n_f is the number density of f in matter, and we have taken into account the fact that the number density of u quarks and d quarks are three times as that of electrons. The constraint on $\epsilon_{\alpha\beta}$ can be summarized as[6; 7]

$$\begin{pmatrix} |\epsilon_{ee}| < 4 \times 10^0 & |\epsilon_{e\mu}| < 3 \times 10^{-1} & |\epsilon_{e\tau}| < 3 \times 10^0 \\ & |\epsilon_{\mu\mu}| < 7 \times 10^{-2} & |\epsilon_{\mu\tau}| < 3 \times 10^{-1} \\ & & |\epsilon_{\tau\tau}| < 2 \times 10^1 \end{pmatrix} \quad \text{at } 90\%\text{CL}. \tag{5}$$

From Eq. (5) we see that $\epsilon_{e\mu} \simeq \epsilon_{\mu\mu} \simeq \epsilon_{\mu\tau} \simeq 0$ is satisfied.

2 Parametrizations in solar and atmospheric neutrino analyses

In Ref. 5 it was shown that the atmospheric neutrino measurements at Hyper-Kamiokande (HK) has a very good sensitivity to the NSI, on the assumptions that (i) all the $\epsilon_{\alpha\mu}$ components of the NSI vanish and (ii) the condition

$$\epsilon_{\tau\tau} = \frac{|\epsilon_{e\tau}|^2}{1 + \epsilon_{ee}} \tag{6}$$

is satisfied, as is suggested by the high energy atmospheric neutrino data.[9] In this talk we discuss the sensitivity of the atmospheric neutrino measurements at HK to NSI without the assumptions (i) and (ii) mentioned above. In Ref. 4, the effect of NSI on solar neutrinos, the 3×3 Hamiltonian in the Dirac equation Eq. (1) with the matter potential (4) is reduced to an effective 2×2 Hamiltonian given by

$$H^{\text{eff}} = \frac{\Delta m_{21}^2}{4E} \begin{pmatrix} -\cos 2\theta_{12} & \sin 2\theta_{12} \\ \sin 2\theta_{12} & \cos 2\theta_{12} \end{pmatrix} + \begin{pmatrix} c_{13}^2 A & 0 \\ 0 & 0 \end{pmatrix} + A \sum_{f=e,u,d} \frac{N_f}{N_e} \begin{pmatrix} -\epsilon_D^f & \epsilon_N^f \\ \epsilon_N^{f*} & \epsilon_D^f \end{pmatrix}, \tag{7}$$

where ϵ_D^f and ϵ_N^f are linear combinations of the standard NSI parameters:

$$\epsilon_D^f = -\frac{c_{13}^2}{2}\left(\epsilon_{ee}^f - \epsilon_{\mu\mu}^f\right) + \frac{s_{23}^2 - s_{13}^2 c_{23}^2}{2}\left(\epsilon_{\tau\tau}^f - \epsilon_{\mu\mu}^f\right)$$
$$+ c_{13}s_{13}\text{Re}\left[e^{i\delta_{\text{CP}}}\left(s_{23}\epsilon_{e\mu}^f + c_{23}\epsilon_{e\tau}^f\right)\right] - \left(1 + s_{13}^2\right)c_{23}s_{23}\text{Re}\left[\epsilon_{\mu\tau}^f\right] \tag{8}$$
$$\epsilon_N^f = -c_{13}s_{23}\epsilon_{e\tau}^f$$
$$+ c_{13}c_{23}\epsilon_{e\mu}^f + s_{13}c_{23}s_{23}e^{-i\delta_{\text{CP}}}\left(\epsilon_{\tau\tau}^f - \epsilon_{\mu\mu}^f\right) + s_{13}e^{-i\delta_{\text{CP}}}\left(s_{23}^2\epsilon_{\mu\tau}^f - c_{23}^2\epsilon_{\mu\tau}^{f*}\right), \tag{9}$$

---

[a] Some models predict large non-standard interactions[8], and hence such large NSI effects are worth investigating also from the view point of model building.

and $c_{jk} \equiv \cos\theta_{jk}$, $s_{jk} \equiv \sin\theta_{jk}$. In the analysis of Ref. 4, one particular choice of $f = u$ or $f = d$ was taken at a time because of the nontrivial composition profile of the Sun.

Since the parametrization which is used in Ref. 4 is different from the one in (2) in the three flavor basis, a non-trivial mapping is required to compare the results in these two parametrizations. It is instructive to see how the two parametrizations are related. Here let us assume for simplicity that $\theta_{13} = 0$, $\theta_{23} = \pi/4$, $\epsilon_{\alpha\mu} = 0$ and $\epsilon_{\tau\tau} = |\epsilon_{e\tau}|^2/(1 + \epsilon_{ee})$, although in our numerical analysis we do not assume these conditions. Then, noting that $\epsilon_{\alpha\beta} = 3\epsilon_{\alpha\beta}^d$ and $\epsilon_D = \epsilon_D^d$, $\epsilon_N = \epsilon_N^d$, Eqs. (8) and (9) become

$$3\epsilon_D = -\frac{1}{2}\epsilon_{ee} + \frac{|\epsilon_{e\tau}|^2}{4(1 + \epsilon_{ee})}, \quad 3\epsilon_N = -\frac{1}{\sqrt{2}}\epsilon_{e\tau}. \tag{10}$$

From Eq. (10) we have

$$\epsilon_{e\tau} = -3\sqrt{2}\epsilon_N, \quad \epsilon_{ee} = -\frac{1}{2} - 3\epsilon_D + \left\{(\frac{1}{2} - 3\epsilon_D)^2 + |3\epsilon_N|^2\right\}^{1/2}, \tag{11}$$

where the sign in the solution in the quadratic equation for $\epsilon_{ee} = 0$ was chosen so that the standard case ($\epsilon_D = \epsilon_N = 0$) is reduced to $\epsilon_{ee} = 0$.

The matter potential (4) with $\epsilon_{\alpha\mu} = 0$ and $\epsilon_{\tau\tau} = |\epsilon_{e\tau}|^2/(1 + \epsilon_{ee})$ can be diagonalized as

$$A \begin{pmatrix} 1 + \epsilon_{ee} & 0 & \epsilon_{e\tau} \\ 0 & 0 & 0 \\ \epsilon_{e\tau}^* & 0 & |\epsilon_{e\tau}|^2/(1 + \epsilon_{ee}) \end{pmatrix}$$

$$= A\, e^{i\gamma\lambda_9} e^{-i\beta\lambda_5} \mathrm{diag}\left\{1 + \epsilon_{ee} + |\epsilon_{e\tau}|^2/(1 + \epsilon_{ee}), 0, 0\right\} e^{i\beta\lambda_5} e^{-i\gamma\lambda_9}, \tag{12}$$

where

$$\tan\beta \equiv \frac{|\epsilon_{e\tau}|}{1 + \epsilon_{ee}}, \quad \gamma \equiv \frac{1}{2}\mathrm{arg}\,(\epsilon_{e\tau}), \quad \lambda_5 \equiv \begin{pmatrix} 0 & 0 & -i \\ 0 & 0 & 0 \\ i & 0 & 0 \end{pmatrix}, \quad \lambda_9 \equiv \begin{pmatrix} 1 & 0 & 0 \\ 0 & 0 & 0 \\ 0 & 0 & -1 \end{pmatrix}.$$

The quantity $\tan\beta$ which is expressed by the matter angle β can be regarded as the gradient of the straight line $|\epsilon_{e\tau}| = (1 + \epsilon_{ee})\tan\beta$ as we can see in the left panel in Fig.1.

In the present case, from (11) we have

$$\tan\beta = \frac{\left|3\sqrt{2}\epsilon_N\right|}{1/2 - 3\epsilon_D + \left\{(1/2 - 3\epsilon_D)^2 + |3\epsilon_N|^2\right\}^{1/2}}. \tag{13}$$

Now if we introduce a new angle

$$\tan\beta' \equiv \frac{\tan\beta}{\sqrt{2}} = \frac{|3\epsilon_N|}{1/2 - 3\epsilon_D + \left\{(1/2 - 3\epsilon_D)^2 + |3\epsilon_N|^2\right\}^{1/2}}, \tag{14}$$

then from Eq. (14) we obtain

$$\tan 2\beta' = \frac{2\tan\beta'}{1 - \tan^2\beta'} = \frac{|3\epsilon_N|}{1/2 - 3\epsilon_D}. \tag{15}$$

Eq. (15) implies that the allowed region of the atmospheric neutrino experiment with the parabolic relation (6) is approximately the one surrounded by the $\epsilon_N = 0$ axis and the straight line $|\epsilon_N| = |\tan 2\beta'||1/6 - \epsilon_D|$ with the gradient $|\tan 2\beta'|$ and the x-intercept $\epsilon_D = 1/6$.

The constraint from the atmospheric neutrino experiments can be expressed as[5]

$$\left|\frac{\epsilon_{e\tau}}{1 + \epsilon_{ee}}\right| \lesssim 0.6 \quad \text{at } 90\%\text{CL}. \tag{16}$$

Combining the constraints (5) and (16), the current allowed region, without assuming that the NSI accounts for the solar neutrino and KamLAND data, is approximately given by the shaded area in the $(\epsilon_{ee}, |\epsilon_{e\tau}|)$-plane (the $(\epsilon_D, |\epsilon_N|)$-plane) in left (right) panel in Fig.1.
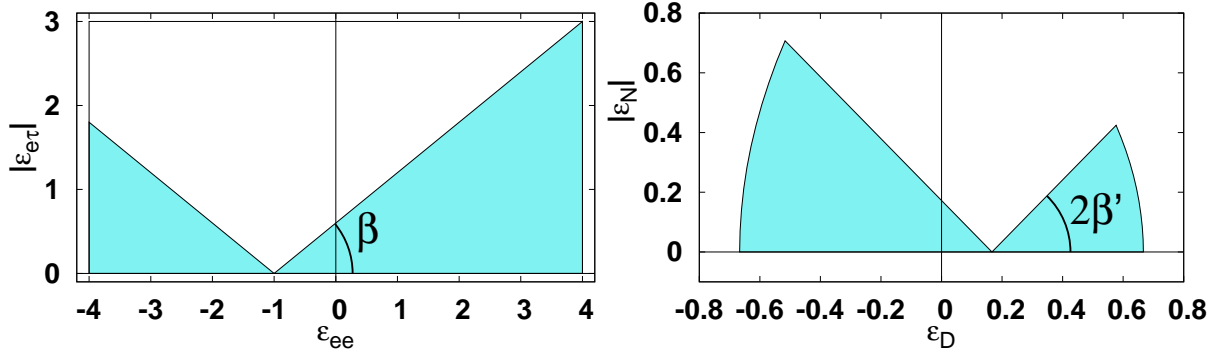
Figure 1 – The current allowed regions in the $(\epsilon_{ee}, |\epsilon_{e\tau}|)$ plane (left panel) and in the (ϵ_D, ϵ_N) (right panel). The region $\epsilon_D > 1/6$ $(< 1/6)$ in the right panel corresponds to $\epsilon_{ee} < -1$ (> -1) in the left panel. The left (right) edge $\epsilon_{ee} = -4$ $(\epsilon_{ee} = 4)$ in the left panel corresponds to the quadratic curve on the right (left) end in the right panel.

3 Results

We performed a χ^2 analysis of the HK atmospheric neutrino experiment, assuming that HK measures the atmospheric neutrinos with the fiducial volume 0.56 Mton for 20 years. We also assumed that the experimental numbers of events are those with the standard three flavor oscillation parameters. From the deviation from the numbers of events with the standard oscillation scenario we have obtained the allowed region for NSI in the $(\epsilon_D, |\epsilon_N|)$ plane. The results are shown in Fig. 2 in the case of both mass hierarchies, assuming that we know the mass hierarchy.[b] The best fit values $(\epsilon_D^d, \epsilon_N^d) = (-0.12, -0.16)$ for NSI with $f = d$ from the solar neutrino and KamLAND data given by Ref. 4 is excluded at 11σ (8.2σ) for the normal (inverted) hierarchy. In the case of NSI with $f = u$, the best fit value $(\epsilon_D^u, \epsilon_N^u) = (-0.22, -0.30)$ is far from the standard scenario $(\epsilon_D, \epsilon_N) = (0.0, 0.0)$ compared with the case of $f = u$ and also excluded at 38σ (35σ) for the normal (inverted) hierarchy. On the other hand, the best fit value from the global analysis of the neutrino oscillation data[4] $(\epsilon_D^d, \epsilon_N^d) = (-0.145, -0.036)$ for NSI with $f = d$ is excluded at 5.0σ (3.7σ) for the normal (inverted) hierarchy. In the case of NSI with $f = u$, the best fit value $(\epsilon_D^u, \epsilon_N^u) = (-0.140, -0.030)$ is excluded at 5.0σ (1.4σ) for the normal (inverted) hierarchy.

4 Conclusion

In this talk we have presented the sensitivity of the future HK atmospheric neutrino experiment to NSI which is suggested by the tension between the mass squared differences from the solar neutrino and KamLAND data. If there are no non-standard interactions in nature, then the best fit point of the combined analysis of the solar neutrino and KamLAND data by Ref. 4 can be excluded at more than 11σ (8σ) in the case of the normal (inverted) hierarchy, while the best fit point of the global analysis in Ref. 4 can be excluded at 5.0σ (1.4σ) in the case of the normal (inverted) hierarchy.

In the HK experiment, because of large statistics, it is expected that the solar neutrino observation, whose typical energy is low ($E_\nu \sim$ several MeV), can test the tension between the solar and KamLAND data by the day night effect.[10] On the other hand, our result indicates that this tension can be tested also by the atmospheric neutrino observation, whose typical energy is high ($E_\nu \sim \mathcal{O}(10)$ GeV), through the matter effect at the same HK facility.

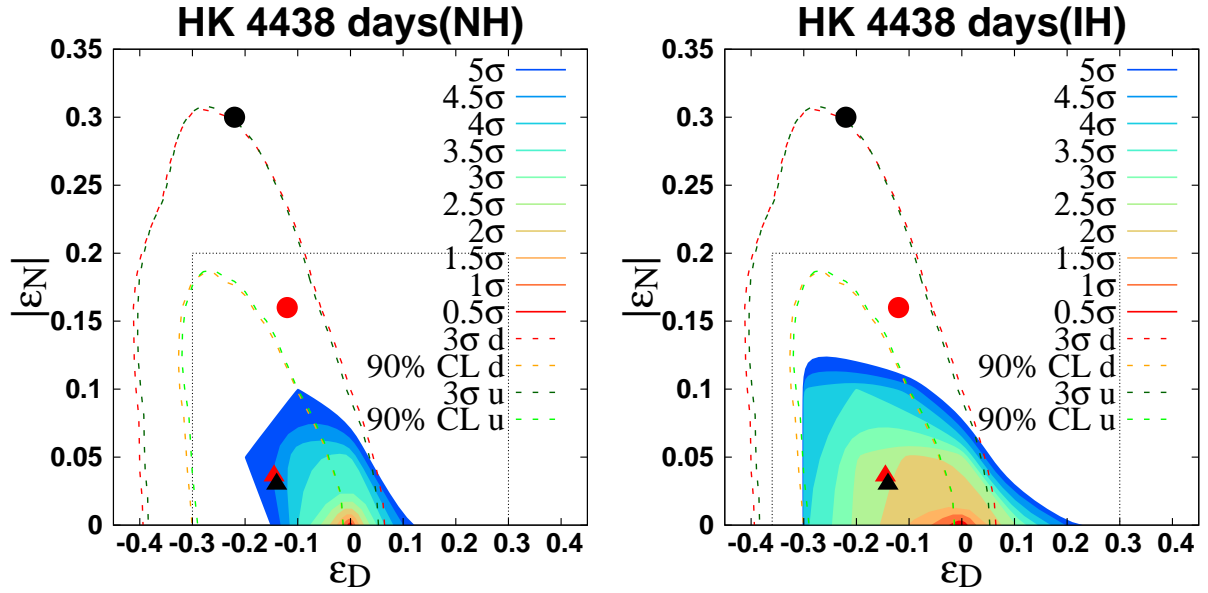[b] The details of our analysis can be found in Ref. 5.

Figure 2 – The allowed region in the $(\epsilon_D, |\epsilon_N|)$ plane from the HK atmospheric neutrino data for the normal hierarchy (left panel) and for the inverted hierarchy (right panel). We calculated χ^2 for $(\epsilon_D, |\epsilon_N|)$ inside the area surrounded by dotted lines and at the best fit points. The red $(f = d)$ and black $(f = u)$ circles indicate the best fit point from the solar neutrino and KamLAND data for NSI with $(\epsilon_D^d, \epsilon_N^d) = (-0.12, -0.16)$ (red) and that for NSI with $(\epsilon_D^u, \epsilon_N^u) = (-0.22, -0.30)$ (black), respectively. The red and black triangles indicate the best fit value from the global neutrino oscillation experiments analysis for NSI with $(\epsilon_D^d, \epsilon_N^d) = (-0.145, -0.036)$ (red) and that for NSI with $(\epsilon_D^u, \epsilon_N^u) = (-0.140, -0.030)$ (black), respectively. The dashed lines are the boundaries of the allowed regions from the global neutrino oscillation experiments analysis. For reference, we plotted for both the cases with $f = u$ and $f = d$.

References

1. K. Abe *et al.* [Hyper-Kamiokande Working Group Collaboration], arXiv:1412.4673 [physics.ins-det].
2. R. Acciarri *et al.* [DUNE Collaboration], arXiv:1512.06148 [physics.ins-det].
3. K. Abe *et al.*, arXiv:1109.3262 [hep-ex].
4. M. C. Gonzalez-Garcia and M. Maltoni, JHEP **1309**, 152 (2013) doi:10.1007/JHEP09(2013)152 [arXiv:1307.3092].
5. S. Fukasawa and O. Yasuda, Adv. High Energy Phys. **2015**, 820941 (2015) doi:10.1155/2015/820941 [arXiv:1503.08056 [hep-ph]].
6. S. Davidson, C. Pena-Garay, N. Rius and A. Santamaria, JHEP **0303**, 011 (2003) [arXiv:hep-ph/0302093].
7. C. Biggio, M. Blennow and E. Fernandez-Martinez, JHEP **0908**, 090 (2009) doi:10.1088/1126-6708/2009/08/090 [arXiv:0907.0097 [hep-ph]].
8. Y. Farzan, in these proceedings.
9. A. Friedland and C. Lunardini, Phys. Rev. D **72** (2005) 053009 [arXiv:hep-ph/0506143].
10. T. Kajita, talk at Neutrino Oscillation Workshop (NOW2016), 4 – 11 September, 2016, Otranto, Italy.